

## Comparison of some thermographic techniques applied to thermal properties characterization of porous materials

by P. Bison, A. Bortolin, G. Cadelano, G. Ferrarini and E. Grinzato

ITC-CNR, Corso Stati Uniti 4, 35127 Padova Italy, [paolo.bison@itc.cnr.it](mailto:paolo.bison@itc.cnr.it)

### Abstract

Several techniques to characterize thermal properties had been developed by using photothermal methods and IR thermography in particular. Some of them are applied in this work on specimens of different building materials, comparing the results and trying to give a correct uncertainty evaluation for each of them. Thermographic measurements are complemented with specific heat by differential scanning calorimeter and volumic mass measurements.

### 1. Introduction

Building materials are more and more required to be characterized by their thermal properties. Depending on the application a building material is sought for a low thermal conductivity in such a way to guarantee a good thermal insulation; sometimes effusivity is the parameter to be minimized, in such a way to drive the system as fast as possible; in other situation a high thermal capacity is advised to guarantee smooth temperature variation when boundary conditions change. In general, when transient conditions are considered, diffusivity and effusivity are the thermal parameters that play the game, and they should be considered more carefully, instead of thermal conductivity as for energetic considerations.

Many techniques that utilize thermography had been developed and tested in our laboratory. The aim of this work is that to apply some of them to the same specimens of building materials trying to draw some conclusion on the accuracy and precision of each of them and on the easiness of the experimental feasibility, both in lab and in-situ.

Among the dynamic measurements of diffusivity the well-known flash method in transmission mode [1] is applied to specimens of thickness around 1 cm. The choice of a relatively large thickness is necessary to obtain specimen representative of the real material used in the field, characterized by large porous size. Indeed, very often the building materials are heterogeneous with components whose diameter is of the order of 1 mm or more. With such a thickness and with a thermal diffusivity generally lower than  $1.0 \times 10^{-6} \text{ m}^2/\text{s}$ , the heating pulse duration must be of the order of some second to obtain a measurable signal on the rear face. At the same time a relatively long duration of the experiment allows the heat exchange with the environment to take place. Therefore a variation of the Parker's model [1] is adopted on the purpose to take into account the finite duration of the heating pulse and the heat exchange with the environment.

Another dynamic approach to measure diffusivity in a one-side (reflection) scheme is to shoot a laser pulse (1 ms duration) on the surface of the specimen with a spatial top-hat shape (1 cm diameter) and measure heat diffusion on the surface [2,3]. Discrete Cosine Transform is used to analyze the spatial shape variation of surface temperature in time. A spatial calibration of the IR camera is necessary to obtain quantitative results. The outcomes are compared to those obtained with the previous technique and critically analyzed from the point of view of the related uncertainties.

Effusivity is measured by using a reference method [4]. A specimen of known effusivity is heated on its surface by a lamp using a step heating function. Next to the reference the unknown specimen is laid down. Both are coated with the same painting on the surface, in such a way to absorb the same amount of specific heating power. Comparing the temperature increasing the effusivity of the unknown sample is obtained.

A steady state measurement of thermal conductivity is carried out by means of two thermoelectric devices (*Peltier* cell) sandwiching a specimen 1 cm thick. One cell works in cooling regime and the other in heating regime generating a steady temperature gradient between the two faces of the specimen. The thermal conductivity of the specimen is obtained by evaluating the heating flux produced by the *Peltier* cell and crossing through the sample section, while temperature is carefully monitored by IR thermography, the contact resistance and the reaching of the steady regime, as well [5].

Finally, a variation of the aforementioned experimental set-up is used in periodic regime [6]. The sample sandwiched between the *Peltier* devices is alternatively cooled and heated with a periodic function. Thermal waves are generated. Their wavelength is proportional to the period of the heating-cooling function and to the thermal diffusivity. The wavelength of the thermal wave is measured after a suitable spatial calibration of the IR camera and by knowing the period of heating-cooling function, the diffusivity of the sample is obtained.

Two more complementary measurements are carried out: volumic mass (density) and specific heat. The first is obtained measuring the weight and volume of a possibly large specimen or averaging the results of several specimens; the second by a Differential Scanning Calorimeter (DSC) on small quantity (generally less than 1 gr) of powder coming from the milling of a representative sample compound of all its heterogeneous phases.

The work is finalized to obtain a comparison between the various techniques and to rank them on the base of their precision and possibly of their accuracy. On the purpose, the following comparisons will be drawn:

- the three techniques furnishing the thermal diffusivity are compared and ranked on the base of the uncertainties of the results
- the combination of diffusivity and effusivity is evaluated to furnish the thermal conductivity and the product of volumic mass with specific heat
- the thermal conductivity obtained in the previous step (dynamic measurements) is compared with the one coming from the steady technique utilizing the *Peltier* cells
- at the same time the product of volumic mass and specific heat coming from the dynamic techniques is compared with the one coming from the complementary measurements by weight and volume measurement and DSC.

## 2. Material and methods

The techniques mentioned in the introduction have been applied to a piece of old brick coming from the ancient church of S.Vito alla Rivera (XIV century) in the town of l'Aquila, to be restored after the earthquake of the April 2009. The brick is an element that tiles the internal part of the roof of the church with a pleasant decorative as shown in Fig. 1. The purpose of the characterization is that of evaluating the thermal load of the roof to project the heating/cooling system.

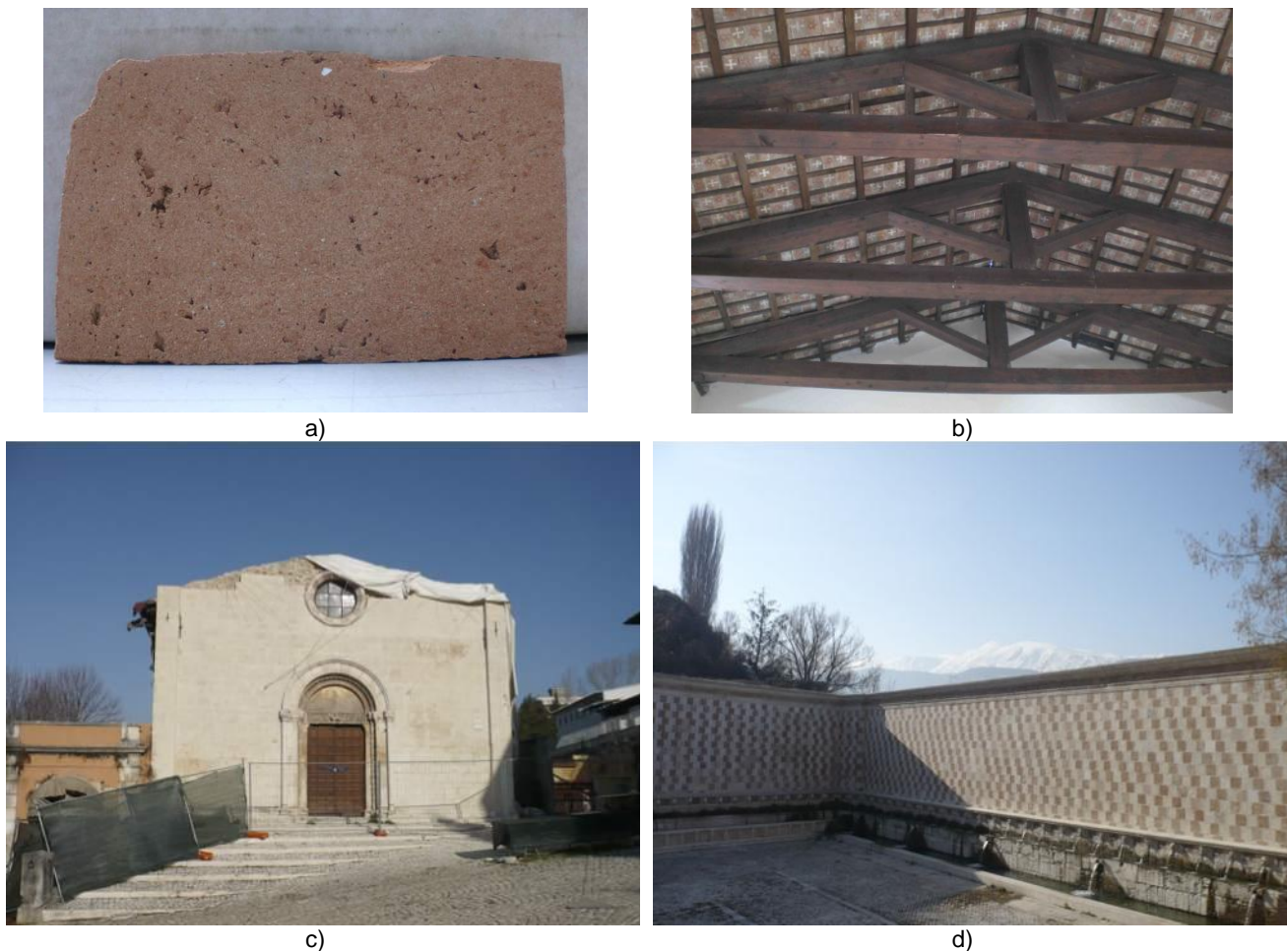


Fig. 1. Image of a piece of clay brick a), coming from the internal decorated roof of the old church of S. Vito alla Rivera in l'Aquila (XIV century) b), the façade c), the "Fontana delle 99 cannelle" in front of the Church d).

### 2.1. Diffusivity measurement

In this work three thermographic methods for the diffusivity measurement are applied.

1) The first method is a transmission method. One face of a slab is heated by a pulse of light produced by switching on and off a halogen lamp. The pulse duration is selected according to the power of the lamp (in our case 1000 W) and to

obtain on the rear face of the specimen a rise in temperature over ambient such that the Signal to Noise ratio is better than 10 (20 dB), possibly around 100 (40 dB). It is applied on the specimen while it is at uniform temperature, equal to ambient. The pulse increases the temperature on the rear face and this increment is followed by the thermographic camera. A sequence of images is grabbed and the temperature rise in time of the rear face is extracted and used in a suitable analytical model that fit the data by a non-linear mean square minimization [7,8] according to:

$$\min_{\mathbf{x}} \|f(\mathbf{x}, t) - data(t)\| \quad (1)$$

where  $t$  is time and  $\mathbf{x}$  is a vector of parameters estimated by the optimization procedure

$$\mathbf{x} = \begin{bmatrix} x_1 \\ x_2 \\ x_3 \end{bmatrix} = \begin{bmatrix} \frac{Q}{h} \\ \frac{a}{L^2} \\ \frac{hL}{\lambda} \end{bmatrix} \quad (2)$$

and the model function  $f(\mathbf{x}, t)$  is given by the analytical solution of the heat equation for a slab of thickness  $L$  [m], exchange with the environment by a coefficient  $h$  [ $Wm^{-2}K^{-1}$ ], thermal diffusivity  $\alpha$  [ $m^2s^{-1}$ ], thermal conductivity  $\lambda$  [ $Wm^{-1}K^{-1}$ ], heated on one side by a specific power  $Q$  [ $Wm^{-2}$ ] for a time  $t_h$  and evaluated on the rear side:

$$f(\mathbf{x}, t) = x_1 \sum_{i=1}^{\infty} 2 \frac{\sin(m_i)}{m_i + \sin(m_i)\cos(m_i)} \exp\left(-x_2 m_i^2 t\right) \exp\left(x_2 m_i^2 t_h\right) - 1 \quad (3)$$

where  $\mu_i^2$  is the  $i$ <sup>th</sup> solution of the transcendental equation  $\mu \operatorname{tg}(\mu) = x_3 = Bi$ , with  $Bi$  the Biot number. In particular, from the estimation of  $x_2$ , by knowing the thickness of slab, the diffusivity is extracted.

2) The second method is a reflection method that analyses the enlargement of a localized spot of light delivered on the surface of the specimen and temporally very short. The method gives the diffusivity of the material provided that the thermal conductivity is a scalar value, i.e. it does not exist a preferential direction of heat diffusion in the material. This technique can be applied also in the field, when it is not possible to obtain a sample slab of the material to test. Indeed it works when a slab is available and with a thick (semi-infinite approximation) material as well. The IR camera records a sequence of images during the delivering of the light spot and successively follows the spreading of the spot on the surface. Then the images are analyzed by calculating for each one in the sequence the spatial cosine transform (the Fourier transform works as well)  $\theta$ . It is demonstrated that the temporal evolution of each component of the transform, divided by the continuous component, decreases exponentially with a time constant depending on the diffusivity:

$$\log\left(\frac{q(k_n, t)}{q(0, t)}\right) = c(k_n) - ak_n^2 t \quad k_n = \frac{2\rho n}{N \cdot D_x} \quad n = [0 : N - 1] \quad (4)$$

In order to extract the diffusivity the wave vector  $k_n$  must be known and that is possible once it is attributed to the pixel the dimension  $\Delta x$  that it covers on the real world. That implies a spatial calibration.

3) The third method is the Ångström's method revisited by using two peltier devices to heat and cool alternatively the specimen on one end, in such a way to generate thermal waves that propagate along the specimen and that are measured by thermography. The thermal waves along the specimen ( $z$  is distance) are given by the following equations:

$$DT(z, t) = A_0 \exp(-k_0 z) + A_1 \exp(-k_1 z) \sin(\omega t - k_2 z + y)$$

$$DT(z, t) = T(z, t) - T_{env} \quad n = \frac{hp}{Sc_p r} \quad \omega = 2\pi f \quad (5)$$

$$k_0 = \sqrt{2 \frac{h p}{l S}} \quad k_1 = \sqrt{\frac{n + \sqrt{n^2 + \omega^2}}{2a}} \quad k_2 = \sqrt{\frac{n - \sqrt{n^2 + \omega^2}}{2a}}$$

where  $p$  and  $S$  are perimeter and cross section of the specimen in the normal direction with respect to the propagation direction of the thermal wave and  $f$  is the frequency of the oscillation of the peltier cells heating and cooling the

specimen.  $k_0$ ,  $k_1$  and  $k_2$  can be determined from the thermographic data by suitable linear analysis. Once estimated they furnish the diffusivity  $\alpha$  and the parameter  $v$  related to the heat exchange with the environment according to

$$a = \frac{W}{2} \frac{1}{k_1 k_2} \quad n = \frac{W}{2} \frac{k_1^2 - k_2^2}{k_1 k_2} \quad (6)$$

### 2.2. Effusivity measurement

The effusivity measurement is carried out by means of a comparative method. The specimen is heated by switching on a lamp for a certain period. It is known that in case of thick sample (semi-infinite approximation) the temperature on the surface rises as the square root of time by a multiplication factor that depends on absorbed power and inversely on the effusivity according to:

$$T(t) = 2 \frac{Q}{e} \sqrt{\frac{t}{\rho}} \quad e = \sqrt{l r C_p} \quad (7)$$

where  $\varepsilon$  is the thermal effusivity [ $\text{Jm}^{-2}\text{K}^{-1}\text{s}^{-1}$ ] and  $C_p$  is specific heat at constant pressure. Submitting a specimen of known effusivity, and painting the surface of the reference and that of the unknown with the same painting, one is sure that both absorb the same amount of power and therefore the effusivity of the unknown is given by:

$$e_{\text{unknown}} = e_{\text{reference}} \frac{T_{\text{reference}}}{T_{\text{unknown}}} \quad (8)$$

By combining the previous measurement of diffusivity and the effusivity measurement the thermal conductivity and the volumic heat capacity is obtained according to:

$$l = e\sqrt{a} \quad rC_p = \frac{e}{\sqrt{a}} \quad (9)$$

### 2.3. Conductivity measurement

The measurement is carried out by a modification of the hot-cold plate test, obtained by means of peltier cells in steady conditions, monitored by thermography. A parallelepiped sample 1 cm thick is covered on the top and bottom faces with peltier cells that heats it on the top and cools it on the bottom. Thermography check the goodness of the contact and the temperature gradient. By knowledge of the peltier cell characteristics and monitoring by thermography their working temperatures it is possible to evaluate the heat flux produced by the cells and passing through the sample that together with the monitored temperature and the knowledge of the its thickness furnish the thermal conductivity according to:

$$l = \frac{qL}{S(T_{\text{top}} - T_{\text{bottom}})} \quad (10)$$

This measurement should be compared with the value obtained by effusivity and diffusivity combination.

### 2.4. Ancillary measurement

Two ancillary measurement are applied to the material: volumic mass  $\rho$  and specific heat  $C_p$  by Differential Scanning Calorimeter. By combining this measurement with those coming from the three diffusivity techniques, the conductivity is

obtained. It can be compared with the one obtained according to 2.2. and 2.3. Furthermore the volumic heat capacity is also obtained and it can be compared with the one obtained in 2.2.

### 3. Results and uncertainties evaluation

#### 3.1. Diffusivity

1) The diffusivity measurement according to the transmission scheme has been carried out by switching on a lamp of 1000 W on one side of the specimen for around 5 s. After switching off the lamp a screen has been interposed between the lamp and the sample in order to obtain a heating function as similar as possible to a square finite pulse as required by the analytical model of eq. 1). A large block of stone, isothermal with the ambient and screened against the heating source, has been positioned inside the field of view of the thermographic camera. The temperature signal collected on it is subtracted to the signal coming from the heated specimen to decrease the common mode noise that affect the camera sensor in the whole. An example of the signal before and after the subtraction of the reference is given in Fig. 2a, while the data fit is shown in Fig. 2b.

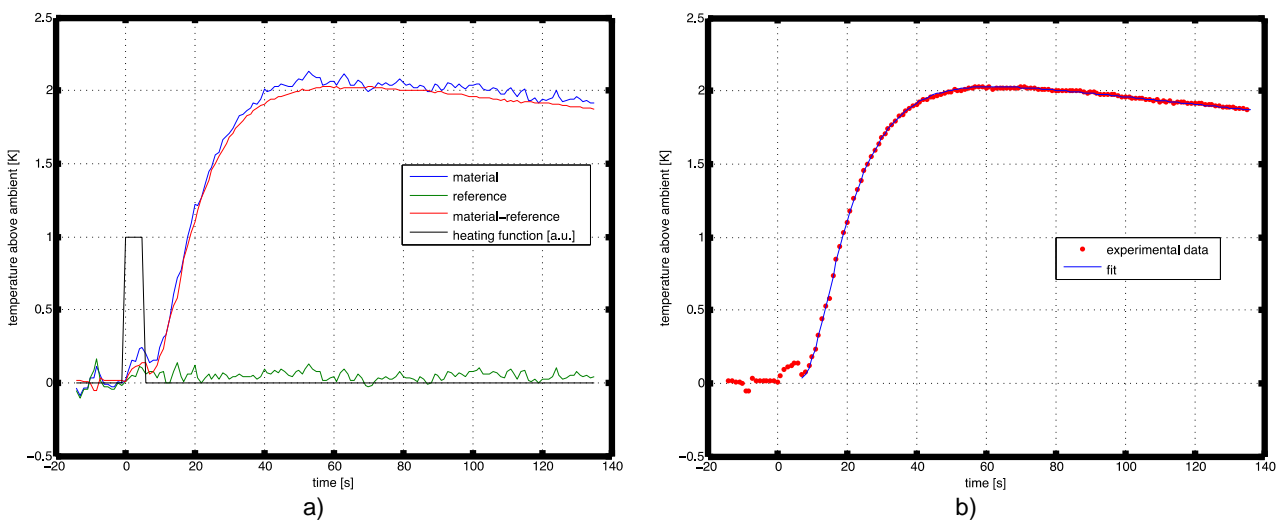


Fig. 2. a) plot of the experimental temperature profiles above ambient; b) plot of the experimental data with the fitting function superimposed

In tab. 1 the results of several measurements are reported. The useful parameter is the average of  $x_2 = \alpha/L^2$  as it comes from 12 different tests. The standard deviation  $\sigma_{x_2}$  is also evaluated. The measurement of the thickness, reported together with its standard deviation  $\sigma_L$ , comes from several measurement on different point of the slab. The diffusivity is eventually computed by multiplying  $x_2$  by the squared thickness and the uncertainty calculated according to the uncertainty propagation rule:

$$a = x_2 L^2 \quad S_a = L S_{x_2} + 2 x_2 L S_L \quad (11)$$

being  $\delta$  the uncertainty of the indicated quantity.

Tab. 1 Diffusivity measurements by the transmission procedure

	$X_2 = \alpha/L^2$ [s <sup>-1</sup> ]	L [m]	$\alpha$ [m <sup>2</sup> s <sup>-1</sup> ]
average	0.0080	0.00787	4.96 E-07
standard deviation	± 0.00022 (± 2.8 %)	± 5E-05 (± 0.6 %)	± 2.01 E-08 (± 4.0 %)

2) The second method to measure diffusivity is carried out by heating the surface of the specimen with a localized pulse of light generated by a laser NdYAG (wavelength 1064 nm). The pulse duration is 500  $\mu$ s and the energy delivered is around 4 J on a circular surface of diameter 1 cm. The IR image immediately after the shot is shown in Fig. 3a. Each image in the sequence is integrated along the rows reducing the image to a line (Fig. 3b). Then, the Fourier Transform is applied to the obtained profile (Fig. 3c). The procedure is repeated for each image and the logarithm of the absolute value of one or more components is plotted against time after normalization with the continuous component of the

Fourier Transform (Fig. 3d). The slope of the fitting line is connected to diffusivity, according to eq. 4. Therefore for diffusivity and its uncertainty we may state the following relations:

$$a = |\text{slope}| \cdot \left(\frac{NDx}{2pn}\right)^2 \quad S_a = \left(\frac{NDx}{2pn}\right)^2 S_{\text{slope}} + 2Dx \left(\frac{N}{2pn}\right)^2 |\text{slope}| S_{Dx} \quad (12)$$

By looking at the absolute value of the FFT, one notices that, a part from the continuous component, the highest value corresponds to the first component. After that, there is a minimum and the 4<sup>th</sup> component is the first noticeable maximum. Indeed the first harmonic component seems to be much affected by experimental conditions, while the 4<sup>th</sup> seems to be much stable, presenting a lower standard deviation among different tests and by choosing different integrating windows (in this case N= 72 pixels) inside the same test. In Tab. 2 the results coming from the 4<sup>th</sup> component (n=4) are presented.

Tab. 2. Results and uncertainty values of diffusivity, from the 4<sup>th</sup> component of the FFT.

	Slope [s <sup>-1</sup> ]	$\Delta x$ [m]	$\alpha$ [m <sup>2</sup> s <sup>-1</sup> ]
average	-0.538	4.0E-4	5.07e-7
standard deviation	$\pm 0.018$ ( $\pm 3.4\%$ )	$\pm 3.2E-05$ ( $\pm 8.0\%$ )	$\pm 9.85 E-08$ ( $\pm 19.4\%$ )

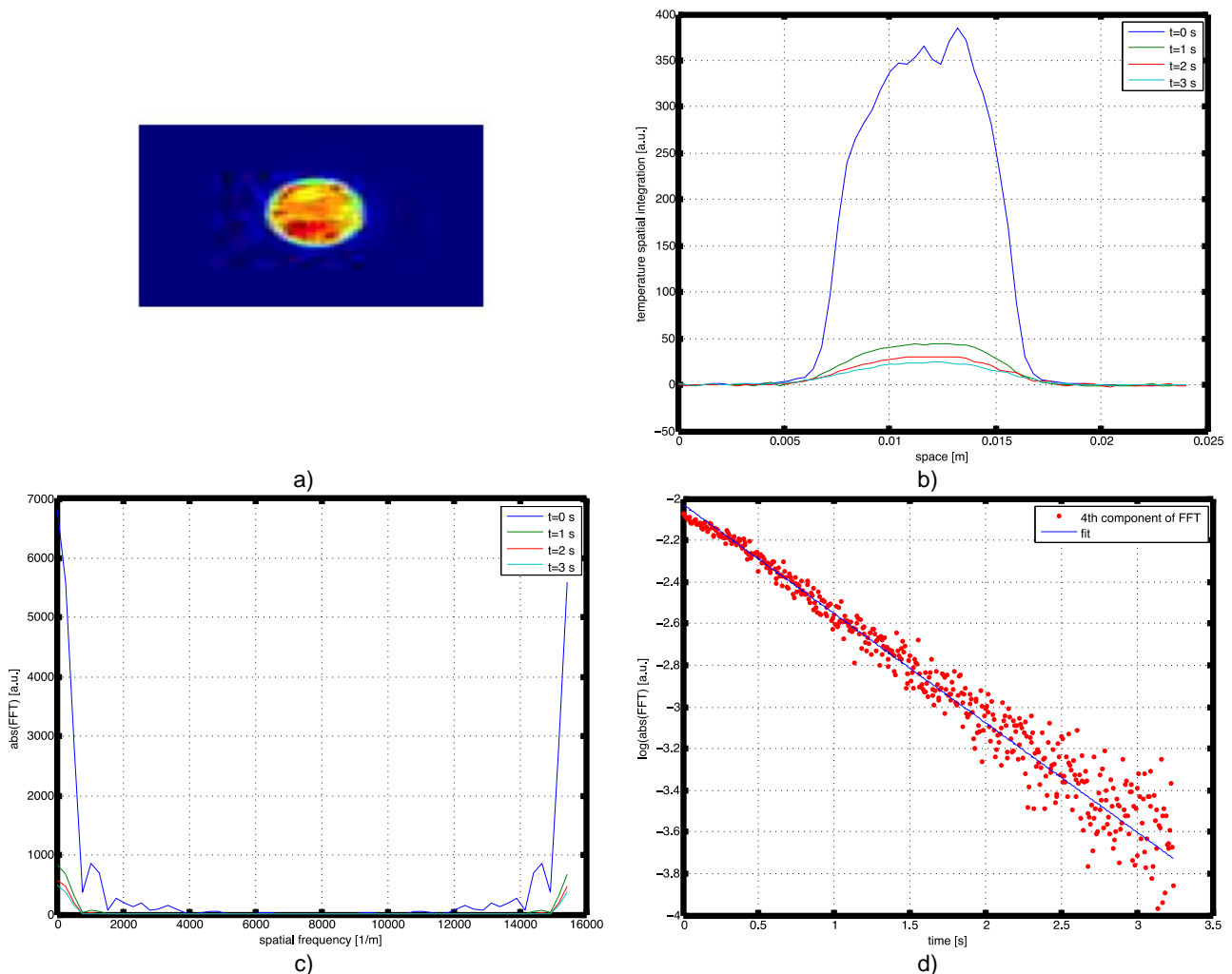


Fig.3. a) IR image of the laser shot on specimen surface; b) by integrating the temperature along the row of the previous image one obtain a profile that evolve in time; c) the Fourier transform is applied to each profile and the absolute value is shown as a function of the spatial frequency; d) the logarithm of the absolute value of the 4<sup>th</sup> spatial frequency component is shown together with the fitting straight line whose slope is proportional to the diffusivity.

3) Two TECs (ThermoElectric Cells) have been driven by a suitable power supply that furnishes a current modulated in a sinusoidal way with a maximum value of around 4 Amp. The two cells sandwich one end of a thin layer of the material under test, leaving the other part of the material free from any source and visible to an IR camera that monitors the thermal waves propagating along the sample. Two tests with period 40 s and 80 s respectively have been carried out. After few minutes the thermal wave reach a steady periodic conditions and the IR camera takes a sequence of images with an acquisition frequency of 1 image/s. 600 images have been grabbed and successively analysed to collect the spatial profile generated by the thermal wave on the surface of the sample at a certain time (see Fig. 4a). Each profile is stacked on a matrix. The sinusoidal behaviour in time of the thermal wave is revealed by reading the matrix along the columns. In the next positions the sinusoidal temperature decreases its amplitude and increases its phase (see Fig. 4b). According to eq. 5) the amplitude decreases as an exponential function of the distance from the source (Fig. 4c), while the phase increases linearly with the distance (Fig. 4d). With suitable fitting one obtains the two constants that allows to determine the diffusivity. Results are reported in Tab. 3.

Tab. 3. Results and uncertainty values of diffusivity, from the thermal waves induced by TEC, period 80 s.

	Slope amplitude	Slope phase	$\alpha$ [m <sup>2</sup> s <sup>-1</sup> ]
average	-317	-265	4.67e-7
standard deviation	± 9 (± 2.8 %)	± 14 (± 5.3 %)	± 3.80 E-08 (± 8.1 %)

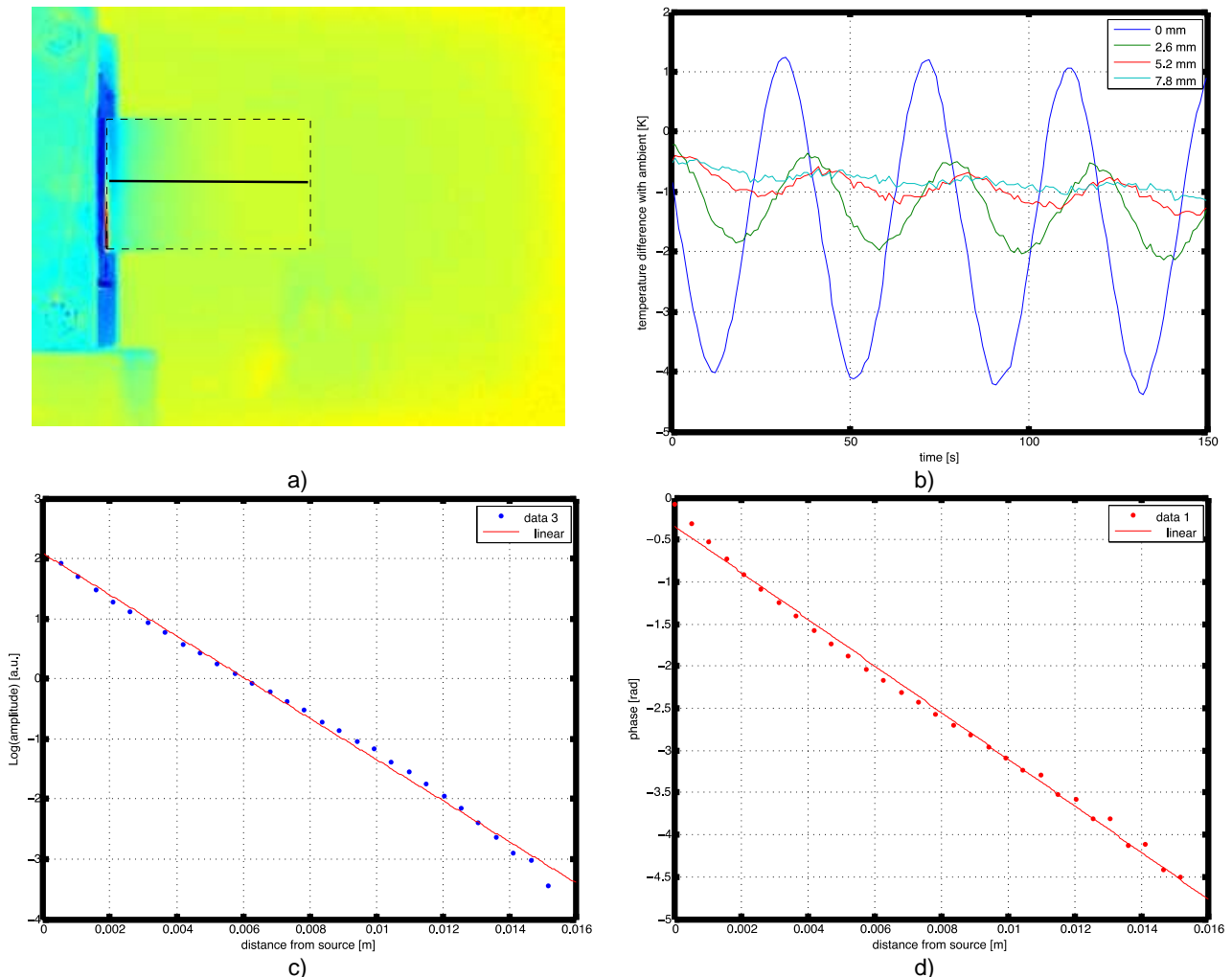


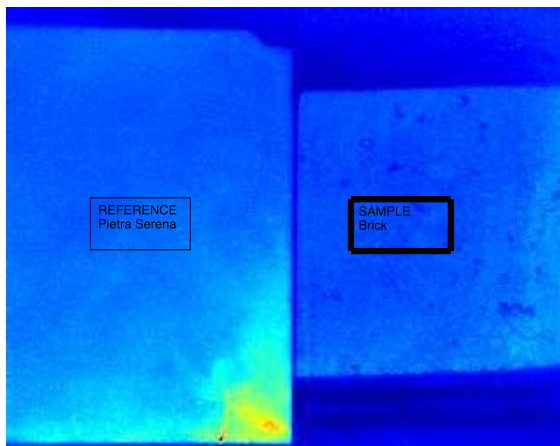
Fig.4. a) IR image of the specimen surface delimited by the dashed rectangle; b) the temperature is analysed in time along the thick central line; c) the logarithm of the temperature amplitude as a function of the distance from source; d) the phase of oscillating temperature as a function of the distance from source.

### 3.2. Effusivity

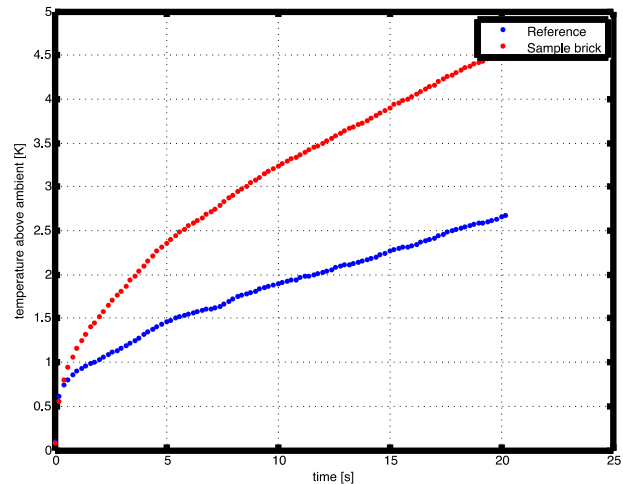
One thick piece of material is laid on a table close to a piece of reference material (pietra serena) whose effusivity is known. The surfaces of the two materials have been milled to make them flat and smooth. Then they have been painted with Graphit 33 (Kontakt Chemie) to make the absorption coefficient as much as possible equal for the two materials. The degree of porosity of the reference material and that of the brick under test are quite different indeed. The surface of the brick shows many large pores ( $\approx 1$  mm diameter, as it is possible to see in Fig. 1a) that make the surface of the brick presumably with a higher absorption than the reference, notwithstanding the same paint used on both the surfaces. An halogen lamp, 1 KW power, is switched on for about some tenths seconds and illuminates the surface of both the samples (Fig. 5a). The increase of temperature is recorded (Fig. 5b) for both the sample. In Fig. 5c the plot of the temperature rise is done against the square root of time in order to obtain straight lines. Two experiments are shown: the first is the same shown in Fig. 5b and the second is the one obtained exchanging the position of the two samples to submit both to the same amount of power in the whole, in case of uneven heating. The ratio between the slopes of reference and sample gives the ratio of the effusivities. The uneven heating is corrected by taking the geometric mean of the two results. Alternatively the ratio between the temperatures can be considered as in Fig. 5d where after a transient the ratio become stable. Two ratio curves are displayed corresponding to the position exchange of the reference and the material under test. Results are reported in Tab. 4.

Tab. 4. Results and uncertainty values of effusivity.

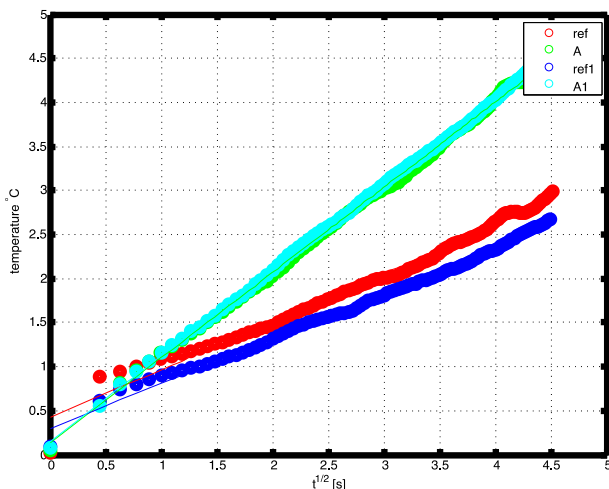
	Effusivity of reference [J m <sup>-2</sup> K <sup>-1</sup> s <sup>-1/2</sup> ]	Ratio (T <sub>brick</sub> /T <sub>ref</sub> )	Effusivity of brick [J m <sup>-2</sup> K <sup>-1</sup> s <sup>-1/2</sup> ]
average	2170	1.71	1270
standard deviation	± 129 (± 6.0 %)	± 0.16 (± 9.6 %)	± 197 (± 15.5 %)



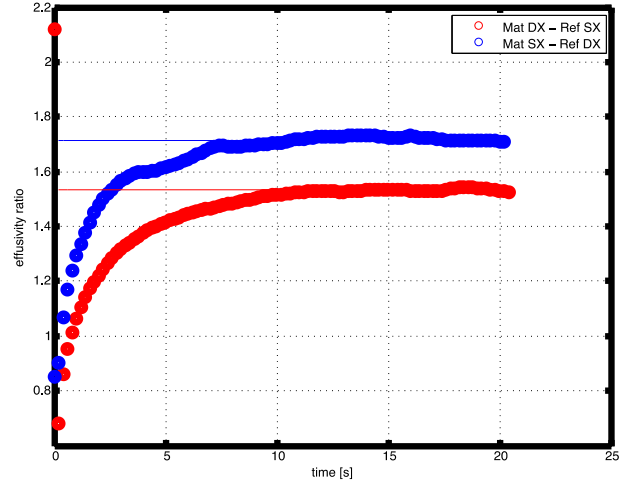
a)



b)



c)



d)

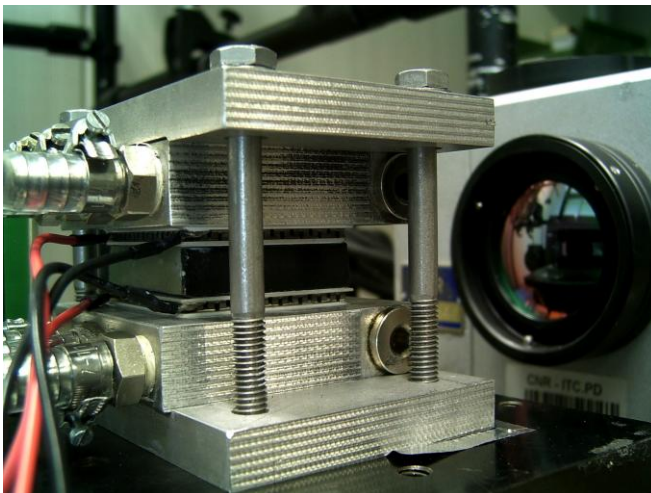
Fig.5. a) IR image of the reference specimen surface and that of brick; b) temperature rises after switching on the lamp with values depending on the effusivity; c) the temperature profiles become straight lines if plotted against the square root of time; d) the ratio of the temperatures collected on the brick and on the reference.

### 3.3. Conductivity

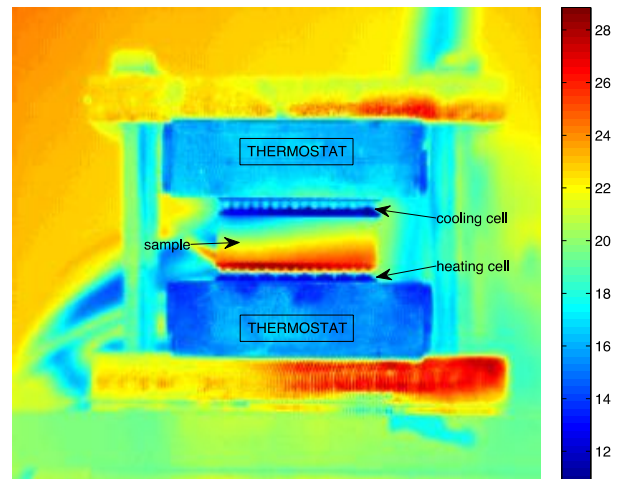
Two TECs, 4 by 4 cms sandwiches a piece of brick of the same dimension, with thickness approximately 1 cm (Fig.6a). One cell heats the sample, the other cools it. The average temperature is around ambient. Thermography, by means of a macro lens, monitors the temperature of the peltier faces to determine the heat flux source/sinked to/from the sample. Moreover, the temperature gradient along the thickness of the sample is considered (Fig.6b). By averaging a suitable number of column on the IR image, a temperature profile is obtained from the top to the bottom. From that, the working temperature of the cells (and so the heat flux) and the temperature gradient on the specimen can be evaluated (Fig. 6c) with the meaning given by the functional scheme of Fig. 6d. Measurements have been done by varying the current driving the peltier cells from 0.3 to 0.7 A with steps of 0.1 A. The results are given in a plot of Fig. 6d. The average value of conductivity and its standard deviation is reported in Tab. 5.

Tab. 5. Results and uncertainty values of conductivity.

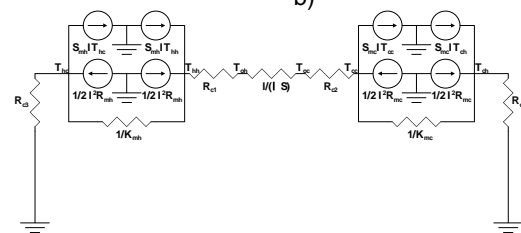
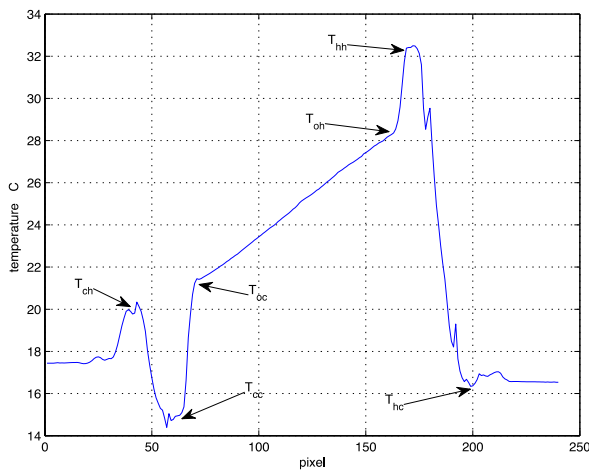
	Conductivity [Wm <sup>-1</sup> K <sup>-1</sup> ]
average	0.76
standard deviation	± 0.01 (± 1.0 %)

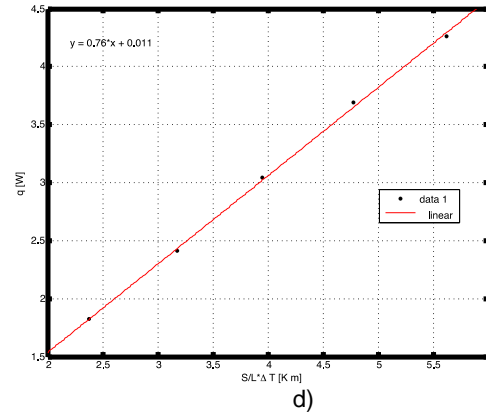


a)



b)





c)

d)

Fig.5. a) experimental lay-out; b) IR image of the device in working conditions ; c) the average temperature profile from top to bottom with indicated the temperature to be considered to evaluate the heat flux and the temperature gradient on the sample; d) a functional scheme of the system: the two block o left and right containing the four current generator correspond to the two thermoelectric cells; the resistance in the middle represent the sample with the two temperatures  $T_{oc}$  on top and  $T_{oh}$  on bottom of the sample. On bottom of Fig.6d the plot of the heat flux vs temperature difference times the area of the sample surface and divided by its thickness. The slope is conductivity.

### 3.4. Ancillary

In the following Tab. 6 the ancillary measurement of volumic mass (density) and specific heat are reported.

Tab. 6. Results and uncertainty values of effusivity.

	Volumic mass [kg m <sup>-3</sup> ]	Specific heat [J kg <sup>-1</sup> K <sup>-1</sup> ]
average	1600	811
standard deviation	± 32 (± 2.0 %)	± 27 (± 3.3 %)

## 4. Discussion and cross reference

The results coming from the diffusivity measurements show that the most precise technique is the one coming from the Parker' s method in transmission mode. Indeed, the other two techniques need a pixel calibration that, if not made with very high accuracy, brings a large uncertainty reflected on the final result. The thermal conductivity is obtained by combining the diffusivity with the ancillary measurements. The same is possible by combining the effusivity and diffusivity and both can be compared with the result coming from the proposed technique that uses the peltier cells. Results are reported in Tab. 7 together with the other possible derived quantity that is heat capacity.

Tab. 7. Derived results for thermal conductivity and heat capacity

	Derived conductivity [W m <sup>-1</sup> K <sup>-1</sup> ]		Derived heat capacity [J m <sup>-3</sup> K <sup>-1</sup> ]
	$l = arC_p$	$l = e \times \sqrt{a}$	$rC_p = e / \sqrt{a}$
Diffusivity 1)	0.64 ±0.06 (± 9.3 %)	0.89 ±0.16 (± 17.6 %)	1801820±316372(±17.6 %)
Diffusivity 2)	0.66 ±0.16 (± 24.7 %)	0.90 ±0.23(± 25.2 %)	1781757±449710(±25.2 %)
Diffusivity 3)	0.61 ±0.08 (± 13.4 %)	0.87 ±0.17(± 19.6 %)	1855964±363607(±19.6 %)

## 5. Conclusion

Several measurements of thermophysical properties have been done on a piece of clayed brick coming from the roof of the Church of S. Vito alla Rivera in L'Aquila, that was damaged after the earthquake on April 2009 and should be restored in the next months. Diffusivity measurements have been carried out by means of three techniques. The one made by transmission mode is the most reliable considering the uncertainty analysis. Combining this result with the measurements of specific heat and volumic mass the most reliable value of thermal conductivity is obtained. The direct measurement of conductivity by using the peltier device in steady state conditions furnishes an apparently better result, if

considering the uncertainty value. But other measurements done on different calibrated material lead us to believe that this steady state measurement is affected by a systematic overestimation of the value. The combination of diffusivity and effusivity measurement lead to a systematic overestimation of both thermal conductivity and heat capacity. This is probably due to the different finishing of the surface of the brick sample and the reference that does not allow to make equal the absorption coefficient by simply painting their surface with the same varnish.

This work shows how important it is to use several different techniques to measure the same parameter. It is presumably the only heuristic method to discover the presence of a systematic error in a measurement technique, that can not be easily discovered by simply repeating the test to improve its statistical significance.

#### ACKNOWLEDGMENTS

This work is partially financed by “Ministero dell’Ambiente e della Tutela del Territorio e del Mare” by means of the project “Pavimento radiante slim per il risparmio energetico”.

#### REFERENCES

- [1] W. Parker, R. Jenkins, C. Butler, and G. Abbott. Flash method of determining thermal diffusivity, heat capacity, and thermal conductivity. *Journal of Applied Physics*, 32(9):1679–1684, 1961.
- [2] I. Philippi, J. Batsale, D. Maillet, and A. Degiovanni. Measurement of thermal diffusivities through processing of infrared images. *Rev. Sci. Instr.*, 66(1), January 1995.
- [3] P. Bison, E. Grinzato, and S. Marinetti. Local thermal diffusivity measurement. *QIRT Journal*, 1(2), 2004.
- [4] P. Bison and E. Grinzato. Building material characterization by using IR thermography for efficient heating systems. In V. P. Vavilov and D. D. Burleigh, editors, *Thermosense XXX*, volume 6939, pages 69390Y–1–9. SPIE, 2008.
- [5] P. Bison and E. Grinzato. Fast estimate of solid materials thermal conductivity by IR thermography. *QIRT Journal*, 7(1):17–34, 2010.
- [6] P. Bison, A. Muscio, and E. Grinzato. Thermal parameters estimation by heating and cooling and thermographic measurement. In D. LeMieux and J. S. Jr., editors, *Thermosense XXI*, volume 3700, pages 402–408. SPIE, 1999.
- [7] MATLAB®, Optimization Toolbox, The Mathworks Inc., 2011.
- [8] Octave's home on the web: <http://www.octave.org>